Acta Neuropathol (2012) 123:273–284
DOI 10.1007/s00401-011-0914-z

ORIGINAL PAPER

Vascular endothelial growth factor induces contralesional corticobulbar plasticity and functional neurological recovery in the ischemic brain

Raluca Reitmeir · Ertugrul Kilic · Barbara S. Reinboth · Zeyun Guo · Ayman ElAli · Anil Zechariah · Ülkan Kilic · Dirk M. Hermann

Received: 17 August 2011 / Revised: 8 November 2011 / Accepted: 12 November 2011 / Published online: 23 November 2011

Abstract Vascular endothelial growth factor (VEGF) is a potent angiogenic factor, which also has neuroprotective activity. In view of these dual actions on vessels and neurons, we were interested whether VEGF promotes long distance axonal plasticity in the ischemic brain. Herein, we show that VEGF promotes neurological stroke recovery in mice when delivered in a delayed way starting 3 days after middle cerebral artery occlusion. Using anterograde tract-tracing experiments that we combined with histochemical and molecular biological studies, we demonstrate that although VEGF promoted angiogenesis predominantly in the ischemic hemisphere, pronounced axonal sprouting was induced by VEGF in the contralesional, but not the ipsilesional corticobulbar system. Corticobulbar plasticity was accompanied by the deactivation of the matrix metalloproteinase MMP9 in the lesioned hemisphere and the transient downregulation of the axonal growth inhibitors NG2 proteoglycan and brevican and the guidance molecules ephrin B1/2 in the contralesional hemisphere. The regulation of matrix proteinases, growth inhibitors, and guidance molecules offers insights how brain plasticity is controlled in the ischemic brain.

R. Reitmeir · B. S. Reinboth · Z. Guo · A. ElAli · A. Zechariah · D. M. Hermann (✉)
Department of Neurology, University Hospital Essen, Hufelandstr. 55, 45122 Essen, Germany
e-mail: dirk.hermann@uk-essen.de

E. Kilic
Department of Physiology, Yeditepe University Istanbul, Istanbul, Turkey

Ü. Kilic
Department of Medical Biology, Vakif University Istanbul, Istanbul, Turkey

Keywords Anterograde tract tracing · Axonal sprouting · Ischemic stroke · Guidance cues · Neurovascular remodeling

Introduction

Subsequent to a stroke, the brain tissue undergoes profound remodeling processes composed of finely tuned cell–cell and cell–extracellular matrix (ECM) interactions [35], aiming at the reconstitution of a functional neurovascular system. In the vicinity of a stroke lesion, new vessels are formed [11, 35]. Besides this, the inhibition of axonal growth, which is characteristic to the adult mammalian central nervous system, is suspended [4, 32]. This suggests that in response to stroke ontogenic protein expression programs are reactivated [5].

Vascular endothelial growth factor (VEGF) is a pleiotropic growth factor that is physiologically expressed in the brain mainly by astrocytes and microglia together with its receptors VEGFR2 and VEGFR1 that are predominantly found on endothelial cells [8, 11, 17]. Upon hypoxia and ischemia, VEGF and its receptors are rapidly induced within hours on neurons and glial cells [11]. In the acute phase of ischemic stroke, VEGF exerts multiple actions in the peri-infarct region that include the promotion of neuronal survival [23, 29], angiogenesis [29, 34], and neural progenitor cell proliferation, migration and differentiation [23, 30].

Recent data in non-human primates subjected to circumscribed infarcts of the motor cortex showed that besides associating with neurons throughout the lesioned hemisphere VEGF can also be found in injury-remote neurons of the contralateral motor cortex [21]. Not only VEGF, but also its receptor VEGFR2 is de novo expressed

on lesion-remote motor cortical neurons [22]. This observation raised the question about VEGF's role in the reorganization of ischemic brain tissue. Lesion-remote plasticity is well established in the meantime to contribute to neurological recovery after stroke in rodents [18, 32] and human patients [9, 27].

In view of the unique activities of VEGF in stimulating the survival and proliferation of neurons and endothelial cells, we were interested to know whether VEGF influences long distance axonal plasticity in the ischemic brain. For this purpose, we performed a comprehensive analysis in mice submitted to focal cerebral ischemia, characterizing effects of a post-acute VEGF delivery on neurological recovery, neuronal survival, angiogenesis, and pyramidal tract plasticity using behavioral studies, anterograde tract tracing, histochemical and molecular biological techniques.

Materials and methods

Animal groups

Experiments were performed in accordance with National Institutes of Health Guidelines for the Care and Use of Laboratory Animals with local government approval (Bezirksregierung Düsseldorf, TSG966/08). A total of 124 male C57Bl6/j mice (8–10 weeks, 23–25 g) were submitted to 30 min of left-sided middle cerebral artery occlusion (MCAO). At 72 h post ischemia, mini-osmotic pumps were implanted into the left-sided lateral ventricle. The pumps were filled with 0.9% NaCl (vehicle) or VEGF (0.004 or 0.02 μg/day diluted in 0.9% NaCl). As such, mice were randomly selected from groups housed together in the same cages that had undergone MCAO on the same day. Animal experiments and behavioral tests were done by two different persons, ruling out data bias. The pumps were left in place during the subsequent 4 weeks and then removed (Fig. 1).

Of 124 mice, three mice were excluded from the study because of respiratory abnormalities that developed during the first 3 days after MCAO. After the implantation of mini-osmotic pumps, five mice had to be removed because of complications related to pump insertion. In the following 4 weeks, four mice opened their wound and manipulated their pump. These animals also had to be killed. There were no differences between groups regarding animal dropouts. A total of 112 mice were further analyzed.

One set of mice were used for studies on functional neurological recovery and for analysis of axonal plasticity ($n = 10$ animals per group). For that purpose, mice received anterograde tract tracer injections in both frontal

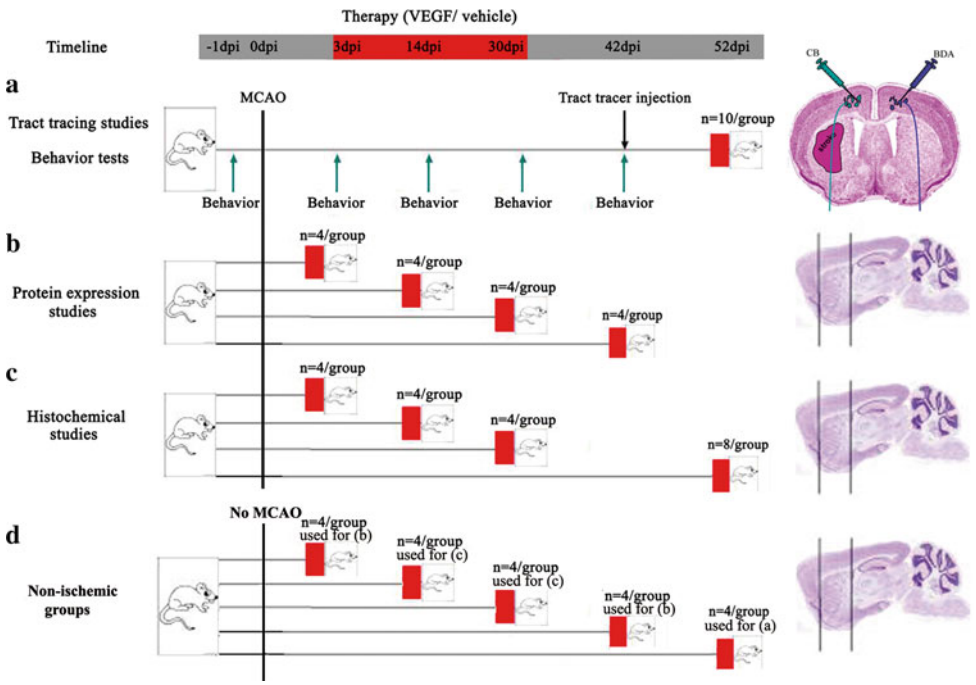

Fig. 1 Experimental procedures and animal groups. Mice submitted to MCAO that were treated with VEGF or vehicle from 3–30 dpi were used for **a** tract-tracing studies and behavioral analysis, **b** protein analysis studies (western blots, gelatin zymography) and **c** conventional histochemical and immunohistochemical studies. Numbers of animals evaluated for each group and time-point of animal killing are shown. On the far right, the rostrocaudal level, from which brain sections and tissue samples were harvested, is also illustrated. In **d**, non-ischemic animals prepared for various experiments in (**a**)–(**c**) are summarized (see also "Materials and methods" section). CB, Cascade blue, BDA, biotinylated dextran amine, dpi, days post ischemia

motor cortices at 42 days after the stroke. Ten days later, the animals were killed (Fig. 1a).

Additional sets of mice were subjected to 30 min MCAO according to the same protocol, followed by implantation of intraventricular pumps filled with vehicle or VEGF (0.02 μg/day in 0.9% NaCl) 3 days later. These animals were killed (1) at 3, 14, 30, or 42 days (used for protein analysis studies, i.e., western blots and gelatin zymography) (Fig. 1b) and (2) at 3, 14, 30, or 52 days (used for histochemistry) (Fig. 1c) after the stroke ($n = 4$ animals per group, survival time and set of animals).

For tract-tracing studies, protein analysis, and histochemistry, additional sham-operated mice receiving pump implantations (filled with vehicle, $n = 4$ per group) (Fig. 1d) were also prepared. In sham-operated animals, the vehicle-filled pumps were implanted as specified. The latter sham-operated and untreated mice were killed at 3, 14, 30, 42, and 52 days post-surgery.

Induction of focal cerebral ischemia

The animals were anesthetized with 1% isoflurane (30% O_2, remainder N_2O). Rectal temperature was maintained between 36.5 and 37.0°C using a feedback-controlled heating system. Cerebral blood flow was analyzed by laser Doppler flow (LDF) recordings. Focal cerebral ischemia was induced using an intraluminal filament technique [7, 13, 33] Shortly, a midline neck incision was made, and the left common and external carotid arteries were isolated and ligated. A microvascular clip was temporarily placed on the internal carotid artery. A silicon-resin-coated nylon monofilament was introduced through a small incision into the common carotid artery and advanced to the carotid bifurcation for MCAO. 30 min later, reperfusion was initiated by monofilament removal. Laser Doppler flow changes were monitored up to 30 min after reperfusion onset. In sham-operated animals, a surgical intervention was performed, in which the neck was opened and the common carotid artery was exposed, but left intact, while LDF recordings were performed. After the surgery, wounds were carefully sutured, anesthesia was discontinued and the animals were placed back into their cages.

Intraventricular pump implantation

Three days after surgery animals were re-anesthetized with 1% isofluran (30% O_2, remainder N_2O) and cannulae linked to mini-osmotic pumps (Alzet 2004 or 2002; Alzet, Cupertino, CA, USA) filled with 0.9% NaCl or VEGF (0.004 μg or 0.02 μg/day in 0.9% NaCl) were implanted into the left-sided lateral ventricle through a bur hole [14]. These pumps were left in place for up to 4 weeks and then removed.

Functional neurological tests

Functional neurological recovery was assessed using a battery of tests at baseline and on days 3, 14 and 42 after MCAO.

Grip strength test: The grip strength test consists of a spring balance coupled with a Newtonmeter (Medio-Line Spring Scale, metric, 300 g, Pesola AG, Switzerland) that is attached to a triangular steel wire which the animal instinctively grasps. When pulled by the tail, the animal exerts force on the steel wire [25]. The grip strength was evaluated at the right paretic forepaw, the left non-paretic forepaw being wrapped with adhesive tape. Grip strength was evaluated five times on occasion of each test, for which mean values were calculated. From these data, percentage values (post-ischemic vs. pre-ischemic) were computed. Pre-ischemic results did not differ between groups.

RotaRod test: The RotaRod consists of a rotating drum with a speed accelerating from 6 to 40 rpm (Ugo Basile, model 47600, Comerio, Italy), which allows to assess motor coordination skills [24]. Maximum speed is reached after 245 s, and the time at which the animal drops off the drum is evaluated (maximum testing time 300 s). Measurements were performed five times each on the same occasion when grip strength was evaluated. For all five measurements, mean values were computed, from which percentage values (post-ischemic vs. pre-ischemic) were calculated. Pre-ischemic data did not differ between groups.

Delivery of cascade blue-labeled dextran amine (CB) and biotinylated dextran amine (BDA)

The anterograde tract tracer BDA has previously been used to evaluate pyramidal tract plasticity contralateral to the stroke in rats submitted to permanent focal cerebral ischemia [37]. We recently adopted this method to mice, administering two different tracers, CB and BDA, in the motor cortex both ipsilateral (CB) and contralateral (BDA) to the stroke [19]. For this purpose, cranial bur holes were drilled 0.5 mm rostral and 2.5 mm lateral to the bregma, via which deposits of 10% BDA or 10% CB (both 10,000 MW; Invitrogen, Darmstadt, Germany), diluted in 0.01 M phosphate-buffered saline (PBS) at pH 7.2) were placed into the motor cortex by means of microsyringe injections 6 weeks after MCAO. As such, a total volume of 2.1 μl tracer was administered to each animal, which was injected in three equal deposits that were located rostrally, medially and caudally of the bur hole inside the motor cortex. For this purpose, the syringe was inserted into the brain at angles of 45°, 90° and 135° against the midline.

Ten days after the tracer injection, the mice were transcardially perfused with 0.1 M PBS containing 100 I.U.

heparin followed by 4% paraformaldehyde in 0.1 M PBS. Brains were removed and post-fixed overnight in 4% paraformaldehyde in 0.1 M PBS and 5% sucrose and cryoprotected in increasing concentrations of sucrose (5, 10, and 30%) over 3 days. The tissue was then frozen with isopentane and cut into 20 and 40 μm thick coronal cryostat sections that were used for conventional and tract-tracing histochemistry.

Conventional histochemical studies

For conventional immunohistochemistry, animals that were transcardially perfused with 0.9% NaCl at 14, 30 and 52 dpi (days post ischemia) were used. The brains were frozen on dry-ice and cut on a cryostat into 20 μm coronal sections [14]. Brain sections from the level of the bregma (i.e., midstriatum) were fixed in 4% PFA in 0.1 M PBS, rinsed, pre-treated for antigen retrieval with 0.01 M citrate buffer (pH 5.0), again rinsed and immersed for 1 h in 0.1 M PBS containing 0.3% Triton X-100 (PBS-T) and 10% normal donkey serum. The sections were incubated overnight at 4°C with monoclonal mouse anti-NeuN (MAB377; Millipore, Schwalbach, Germany) and rat anti-CD31 (#557355; BD Biosciences, Heidelberg, Germany) antibodies. After detection with Cy3 or Cy2 conjugated secondary antibodies, the sections were incubated with 4′-6-diamidino-2-phenylindole (DAPI) and coverslipped. For the evaluation of DNA fragmentation, adjacent brain sections were stained by terminal transferase dUTP nick end labeling (TUNEL) [13, 14]. The sections were evaluated under a fluorescence microscope (BX 41; Olympus, Hamburg, Germany) connected to a CCD camera (CC12; Olympus). Surviving NeuN + neurons, CD31 + microvessels and DNA-fragmented cells were analyzed in a blinded way by counting numbers of cells or profiles in six defined regions of interests (ROI) per striatum measuring 62,500 μm^2, both ipsi- and contralateral to the stroke [14]. Mean values were calculated for all areas. Striatal atrophy and corpus callosum atrophy were assessed on sections stained with modified Bielschowsky silver solution [6]. Thus, the borders of both structures were outlined and their surface analyzed (in case of corpus callosum up to 1 mm lateral to midline, thus reflecting areas on coronal brain sections [3]).

Immunohistochemistry for CB and BDA

Brain sections of animals that had transcardially been perfused with 4% PFA at 52 dpi were rinsed three times for 10 min each in 50 mM Tris-buffered saline (pH 8.0) containing 0.5% Triton X-100 (TBST). For detection of CB, sections were immersed overnight at 4°C with polyclonal rabbit anti-cascade blue antibody (A-5760; Invitrogen, 1:100), diluted 1:100 in 50 mM TBST, followed by incubation for 1 h at room temperature with a horseradish peroxidase (HRP)-labeled secondary anti-rabbit antibody (1:1,000). For detection of BDA, the sections were incubated overnight with avidin–biotin-peroxidase complex (ABC Elite; Vector Labs). Stainings were revealed with 3,3′-diaminobenzidine (DAB) containing 0.4% ammonium sulfate and 0.004% H_2O_2.

Analysis of corticobulbar projections

The localization of tracer deposits was checked at the levels of the needle tracks, thus ensuring that the motor cortex had indeed been injected in all animals. To account for variabilities in tracer uptake in different mice, we first evaluated the number of tracer-stained fibers in the corticospinal tract (CST) at the level of the facial nucleus. For this purpose, two consecutive sections were analyzed, counting the number of fibers crossing the sections in four regions of interest of 2,865 μm^2 each that had been selected in the dorsolateral, ventrolateral, dorsomedial and ventromedial portion of the CST. By measuring the total area of the CST using the cell software image system (Olympus) connected to an Olympus BX42 microscope, we calculated the overall number of labeled pyramidal tract fibers, as described [19, 37].

Corticobulbar projections were evaluated at the level of the facial nucleus (bregma −5.8 to −6.3 mm). Two 500 μm long intersection lines were superimposed on the sections parallel to the midline, both representing tangents touching the most lateral extension of the pyramidal tract. Along both lines those fibers crossing the lines in direction of the contralateral and ipsilateral facial nucleus were quantified. For each animal, the total number of fibers counted was normalized with the number of labeled fibers in the CST and multiplied with 100, resulting in percent values of fibers originating from the pyramidal tract [19]. For both tracers two consecutive sections were evaluated, of which mean values were determined.

Western blot analysis

For western blotting, tissue samples were harvested from mice killed by decapitation at 3, 14, 30, and 42 dpi. Brains were dissected on dry-ice. Blocks of tissue were cut from 2 mm rostral to 2 mm caudal to the bregma, from which samples were taken from the striatum, motor cortex and parietal cortex both ipsilateral and contralateral to the stroke. Tissues belonging to the same hemisphere and time-point were pooled and homogenized on ice for 30 s, ultrasonicated for 2 min and treated with protease inhibitor cocktail and phosphatase inhibitor cocktail. Protein content was measured using the Bradford method. Equal amounts of protein were loaded on 5% (NG2 proteoglycan), 7%

(brevican) or 10% (ephrin B1, ephrin B2, c-Jun, activated caspase-3) gels, followed by sodium dodecyl sulfate polyacrylamide gel electrophoresis (SDS-PAGE). Proteins were transferred onto PVDF membranes (Bio-Rad, Hercules, CA, USA) that were blocked in 5% nonfat milk in Tris-buffered saline containing 0.1% Tween (TBS-Tw) for 1 h at room temperature, washed in TBS-Tw and incubated overnight with monoclonal rabbit anti-total c-Jun (#9165, Cell Signaling), polyclonal rabbit anti-phospho-c-Jun (#9164S, Cell Signaling), polyclonal rabbit anti-activated caspase-3 (#9661; Cell Signaling), polyclonal rabbit anti-NG2 proteoglycan (H-300, sc-20162; Santa Cruz, Heidelberg, Germany), monoclonal mouse anti-brevican (610895; BD Biosciences), polyclonal rabbit anti-ephrin B1 (H70, sc-20723; Santa Cruz) and polyclonal goat anti-ephrin B2 (AF496; R&D Systems, Wiesbaden, Germany) antibody, diluted 1:1000 in TBS-Tw. The next day membranes were washed and incubated in blocking solution with peroxidase-conjugated secondary antibodies for 1 h at room temperature. Blots were developed using a chemiluminescence kit. The intensity of each signal was measured on a total of three digitized blots each using the Image J software program. Protein loading was controlled by means of β-actin blots using a polyclonal rabbit antibody (#4967, Cell Signaling). The relative levels of proteins were normalized with values determined in the contralateral striatum of animals killed at 3 dpi, i.e., the day when VEGF was administered.

Analysis of matrix metalloproteinase-9 activity by gelatin zymography

Tissue samples from the same animals were processed for matrix metalloproteinase-9 (MMP9) activity using a previously published gelatin zymography protocol [36]. Brain samples were homogenized and lysed in NP-40 lysis buffer (150 mM NaCl, 50 mM Tris–HCl, 1% NP-40, pH 8.0) containing 5% protease inhibitor cocktail. Protein concentration was estimated using the DC Protein Assay Kit using an iMark microplate reader. Samples containing 5 μg protein were subjected to SDS-PAGE using 8% bis-acrylamide gel containing 0.1% gelatin (Sigma, Deisenhofen, Germany). After electrophoresis, gels were incubated for 1 h at room temperature in modified enzymatic activation buffer (MEAB) (50 mM Tris–HCl, 6 mM $CaCl_2$, 1.5 μM $ZnCl_2$, pH 7.4) containing 2.5% Triton X-100, followed by overnight incubation in MEAB. The next day, gels were stained in coomassie brilliant blue R-250. The gels were dried and digitized. A number of three experiments were run for each tissue sample.

Statistical analysis

Behavioral tests were analyzed by means of two-way repeated measurement analysis of variance (ANOVA; treatment x time) at three different time-points starting with 3 days post-stroke, i.e., the time-point when VEGF was administered. For those tests in which significant treatment or treatment by time interaction effects were noticed (at 0.05 level), one-way ANOVA were done for each time-point, using least significant differences (LSD) tests as post hoc tests. Tract-tracing histochemistries were evaluated by oneway ANOVA, followed by LSD tests (comparison between $n \geq 3$ groups). Conventional histochemical stainings, Western blots and gelatin zymographies were analyzed by two-way ANOVA (treatment × time) or two-tailed *t*-tests, as appropriate. Whenever a treatment effect or treatment by time interaction effect was present in two-way ANOVA at the 0.05 level, two-tailed *t*-tests were performed for each time-point as post hoc tests.

Results

Neurological recovery is improved by post-acute VEGF delivery

In order to evaluate if VEGF promotes neurological recovery when administered in the post-acute stroke phase, mice submitted to 30 min of left-sided MCAO were intracerebroventricularly (i.c.v.) treated with vehicle or VEGF (0.004 or 0.02 μg/day) starting at 3 dpi. LDF, which was recorded to evaluate changes in cerebral blood flow (Fig. 2a), and body weight (Fig. 2b) did not reveal any differences between groups. Mean LDF values decreased to 15–20% of baseline values during MCAO, followed by stable reperfusion to levels slightly above pre-ischemic values (Fig. 2a). Only a mild reduction in body weight was noticed at 3 dpi in all groups (∼10%), from which animals quickly recovered within 14 dpi (Fig. 2b).

Motor recovery was investigated by grip strength (Fig. 2c) and Rotarod (Fig. 2d) tests. Reductions in motor force of the contralesional right forelimb (Fig. 2c) and coordination skills (Fig. 2d) were noticed in animals submitted to 30 min MCAO. In vehicle-treated ischemic animals and animals receiving VEGF at low dosage (0.004 μg/day), deficits in motor force and coordination persisted over the observation period of 6 weeks (Fig. 2c, d). In animals treated with 0.02 μg/day VEGF, on the other hand, grip strength and coordination skills progressively improved during that time interval, reaching levels significantly above vehicle-treated animals at 42 dpi (Fig. 2c, d).

VEGF promotes neurovascular remodeling

To assess how VEGF affects neuronal survival, immunohistochemistries against the neuronal marker NeuN were analyzed in mice receiving VEGF at the higher dosage

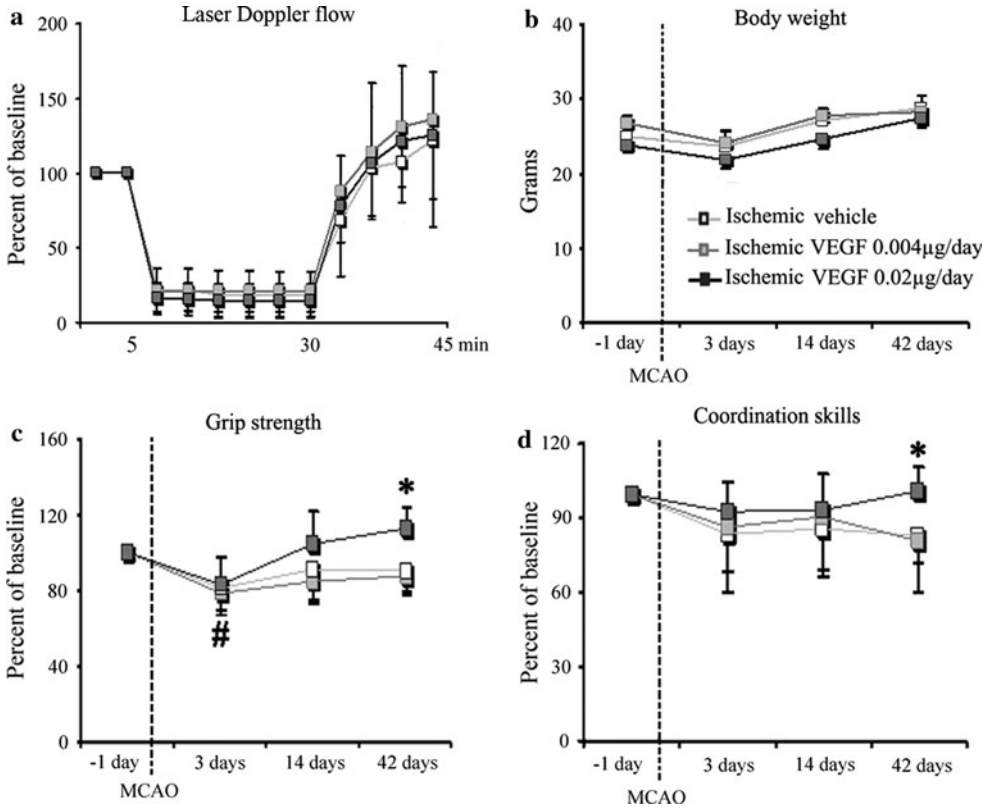

Fig. 2 Delayed delivery of VEGF at 0.02 µg/day, but not 0.004 µg/day promotes post-ischemic neurological recovery. **a** LDF recordings above the core of the MCA territory, **b** body weight, **c** grip strength of the lesion-contralateral right paretic forepaw, and **d** coordination skills evaluated by RotaRod tests. Note that motor force (**c**) and coordination skills (**d**) do not exhibit any major improvements over time in vehicle-treated mice and mice receiving VEGF at a dosage of 0.004 µg/day, but progressively increase over 14 to 42 days in animals treated with 0.02 µg VEGF/day. LDF recordings (**a**) and body weight (**b**) do not differ between groups. Data are mean values ± S.D. ($n = 10$ animals per group). Data were analyzed by two-way repeated measures ANOVA, followed by one-way ANOVA/LSD tests for each time-point. $^{\#}p < 0.05$ compared with pre-ischemic baseline, $^{*}p < 0.05$ compared with vehicle-treated ischemic mice

(0.02 µg/day). Slowly progressive degeneration was noticed in the ischemic striatum of vehicle-treated mice, reflected by a loss of surviving neurons (Fig. 3a) and progressive striatal atrophy (Fig. 3b). Notably, VEGF significantly increased neuronal survival at 14 dpi (Fig. 3a), translating into reduced shrinkage of the ischemic striatum at 52 dpi (Fig. 3b).

As reported previously [23, 29], VEGF significantly increased the density of CD31 + brain capillaries more strongly in the ipsilesional than contralesional striatum (Fig. 3c). The thickness of the corpus callosum, as evaluated by modified Bielschowsky stainings, was slightly, but significantly increased by VEGF (Fig. 3d).

VEGF promotes contralesional corticobulbar plasticity

To analyze how VEGF influences pyramidal tract plasticity, two dextran conjugates, CB and BDA, were administered into both motor cortices. Injection sites were obtained that covered the more caudal forelimb area and rostral hindlimb area of the primary motor cortex. The number of anterogradely labeled axons in the pyramidal tracts did not differ between vehicle-treated and VEGF-treated mice, neither ipsilateral nor contralateral to the stroke (19,188 ± 7,383 vs. 25,408 ± 16,306 fibers on lesioned side for vehicle and VEGF, respectively, at level of facial nucleus). The area covered by the pyramidal tract was also similar in both groups (0.05 ± 0.02 vs. 0.07 ± 0.04 mm^2 on lesioned side/0.06 ± 0.01 vs. 0.07 ± 0.02 mm^2 contralateral to stroke for vehicle and VEGF, respectively), indicating that neither ischemia, nor VEGF influenced the survival of pyramidal tract axons.

Importantly, VEGF promoted the sprouting of labeled fibers branching off the contralesional, but not ipsilesional pyramidal tract in direction to the facial nuclei. As such, the number of labeled midline-crossing fibers originating from the BDA-labeled contralesional pyramidal tract was significantly increased, as was the number of fibers branching off the contralesional pyramidal tract in direction of the contralesional facial nucleus (Fig. 4). Interestingly, VEGF did not affect the plasticity of CB-labeled ipsilesional corticobulbar fibers that was increased

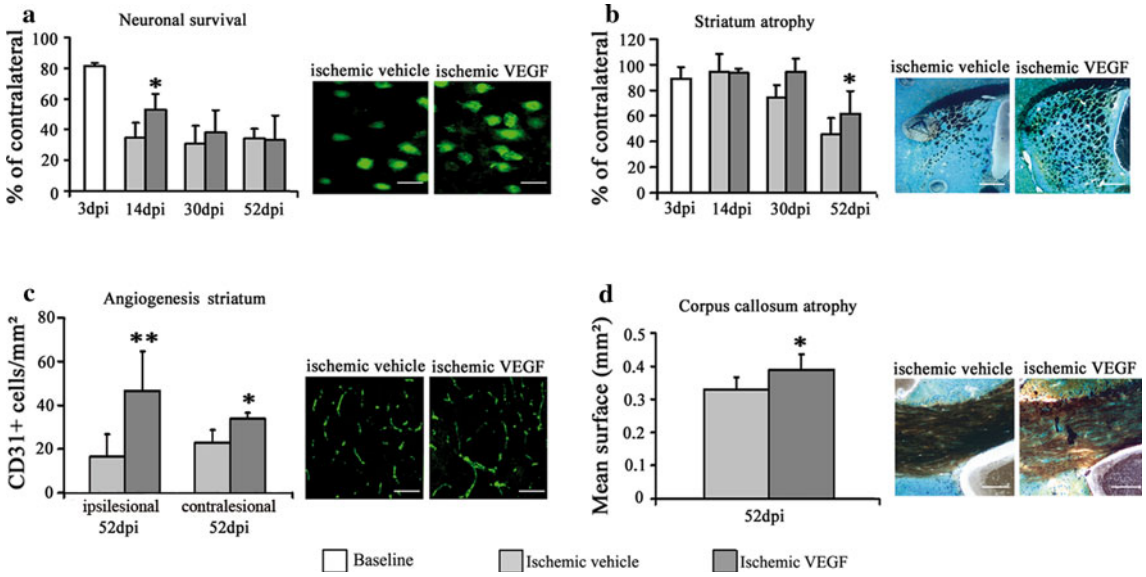

Fig. 3 VEGF promotes neurovascular histological brain remodeling. **a** Density of surviving neurons in ischemic striatum evaluated by NeuN immunohistochemistry, **b** striatal shrinkage examined by Bielschowsky staining, **c** capillary density in ischemic striatum assessed by CD31 immunohistochemistry and **d** corpus callosum atrophy evaluated by Bielschowsky staining. Note that VEGF increases neuronal survival at 14 dpi (**a**) and reduces brain atrophy later on at 52 dpi (**b**). In addition, VEGF promotes angiogenesis (**c**) and mildly increases corpus callosum thickness (**d**). Microphotographs are also shown that were taken at 14 dpi (**a**) or 52 dpi (**b**–**d**). Data are mean values ± S.D. (n = 4-8 animals per group). Data were analyzed by two-way ANOVA followed by two-tailed t-tests for individual time-points or two-tailed t-tests, as appropriate. *$p < 0.05$/**$p < 0.01$ compared with vehicle-treated ischemic mice. *Bar* 200 μm (**b**)/50 μm (**c**, **d**)/20 μm (**a**)

in ischemic as compared with sham-operated non-ischemic mice (Fig. 4).

Brain remodeling involves deactivation of matrix metalloproteinase MMP9 in the ischemic, but not contralesional hemisphere

To elucidate mechanisms underlying the reorganization of the brain tissue both ipsilateral and contralateral to the stroke, we examined the activation of MMP9 by gelatin zymography. Activation of MMP9 was noticed throughout the ischemic hemisphere (i.e., in striatum, parietal cortex and motor cortex) over the observation period of 42 days (shown for striatum in Fig. 5a). VEGF significantly attenuated MMP9 activity (Fig. 5a). Contralateral to the stroke, a mild activation of MMP9 was found at 3 dpi, but not at later time-points (not shown).

VEGF modulates the transcription factor c-Jun and inhibits apoptotic cell death

To characterize mechanisms underlying perilesional tissue remodeling, western blots for the transcription factor c-Jun and the executioner caspase-3 were evaluated using antibodies detecting both total and phosphorylated c-Jun as well as cleaved (i.e., activated) caspase-3 using tissue samples obtained from the ischemic and contralesional non-ischemic striatum. c-Jun was abundant in ischemic brain tissue (Fig. 5b). Although the expression of total (i.e., phosphorylated and non-phosphorylated) c-Jun was downregulated by VEGF in the ischemic (Fig. 5b), but not non-ischemic (not shown) striatum at 14 dpi, VEGF increased the percentage of phosphorylated c-Jun in the ipsilesional brain tissue (Fig. 5b). In accordance with the promotion of neuronal survival, caspase-3 activity was reduced by VEGF in the ischemic striatum at 14 dpi (Fig. 5c), as was DNA-fragmentation evaluated by TUNEL at 14 dpi (Fig. 5d).

VEGF-induced contralesional plasticity is accompanied by the downregulation of growth inhibitory proteoglycans and guidance molecules

To clarify, how VEGF influenced axonal plasticity in the contralesional hemisphere, western blots for the axonal growth inhibitory proteoglycans NG2 and brevican and for the vascular and axonal guidance proteins ephrin B1 and ephrin B2 were analyzed using tissue samples obtained from the lesion-sided and contralesional striatum. In general, the abundance of these four proteins was upregulated in the subacute compared with acute phase of the stroke, particularly at 14 and 30 dpi (Fig. 6). Intriguingly, VEGF did not influence the expression of these proteins in the ipsilesional striatum, which is traversed by descending pyramidal tract axons, but reduced the abundance of NG2, brevican and ephrin B2 in the contralesional striatum at 14 dpi (Fig. 6).

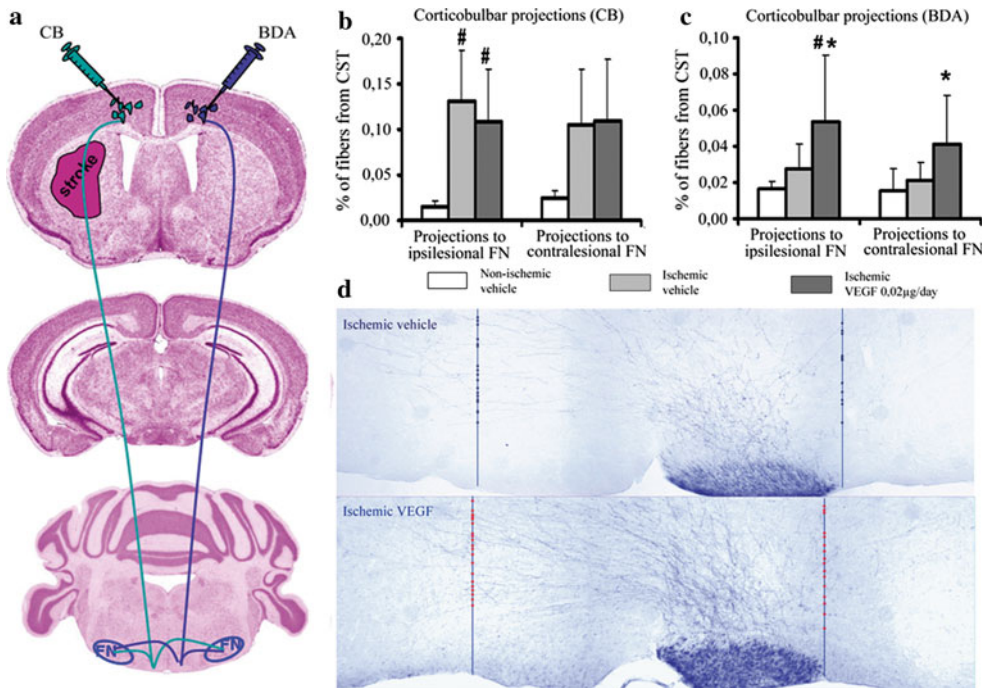

Fig. 4 VEGF promotes contralesional, but not ipsilesional corticobulbar plasticity. Tract-tracing analysis at the level of the facial nucleus (*FN*) in mice receiving cascade blue (*CB*) and biotinylated dextran amine (*BDA*) injections into the lesion-sided and contralesional motor cortex (for placement of tracer injections see (**a**)). Percent of fibers leaving the pyramidal tract in direction to the ipsilesional and contralesional FN traced by (**b**) CB and (**c**) BDA. Note that the percentage of fibers projecting to the ipsilesional FN after CB injection into the lesion-sided motor cortex significantly increases in response to stroke (**b**). Interestingly, VEGF does not further strengthen this ipsilesional projection (**b**), but increases the percentage of BDA stained contralesional pyramidal tract fibers innervating the ipsilesional and contralesional FN (**c**). **d** Microphotographs of representative ischemic vehicle-treated and VEGF-treated mice showing BDA-traced corticobulbar fibers crossing the intersection lines (superimposed in *blue*) on both sides of the brain. Note that VEGF increases axonal sprouting towards both FN (intersecting fibers labeled with dots). Data are means ± S.D. ($n = 10$ animals per group (ischemic vehicle, ischemic VEGF)/$n = 4$ animals per group (non-ischemic vehicle)). Data were analyzed by one way ANOVA followed by LSD tests. $^{\#}p < 0.05$ compared with vehicle-treated non-ischemic mice. $^{*}p < 0.05$ compared with vehicle-treated ischemic mice

Discussion

Using a broad set of behavioral, histochemical and molecular biological techniques, which allowed us to perform a comprehensive analysis of (a) sensorimotor recovery, (b) secondary neurodegeneration in the perilesional tissue, (c) angiogenesis, and (d) corticobulbar plasticity both ipsi- and contralateral to the stroke, this study shows that VEGF delivery promotes long distance axonal sprouting of the contralesional pyramidal tract system and induces functional neurological recovery, when delivered in the post-acute phase of the stroke starting 3 days after focal cerebral ischemia. That VEGF stimulates axonal plasticity has to the best of our knowledge not been shown. Promotion of pyramidal tract plasticity has previously been reported after focal cerebral ischemia following deactivation of the axonal growth inhibitor NogoA [18, 32], delivery of bone marrow-derived stem cells [1] and erythropoietin [19].

Although we used a delayed delivery protocol, upon which VEGF was applied starting at 72 h after the stroke, VEGF promoted structural histological brain remodeling. As such, VEGF protected the brain against delayed neuronal death at 14 dpi, inhibiting caspase-3-dependent apoptotic injury, and prevented post-acute tissue shrinkage at 30 and 52 dpi. Besides, VEGF enhanced angiogenesis in the brain of VEGF-treated mice, as investigated in this study at 52 dpi. The attenuation of brain atrophy highlights the importance of protracted reorganization processes, which continue to progress over several weeks [3, 19]. Delayed neurodegeneration and brain atrophy have previously been reported to be reversed by delivery of neural precursor cells [3] and erythropoietin [19], when these neural precursor cells or erythropoietin were used in a similarly delayed time window. Post-ischemic neuroprotection and angiogenesis have repeatedly been described after acute VEGF delivery [11]. Neuroprotection was noticed as long as the growth factor was locally administered at post-acute time-points (1–3 days post ischemia) [23] or constitutively overexpressed in the brain but not the rest of the body [29], whereas systemic delivery was found

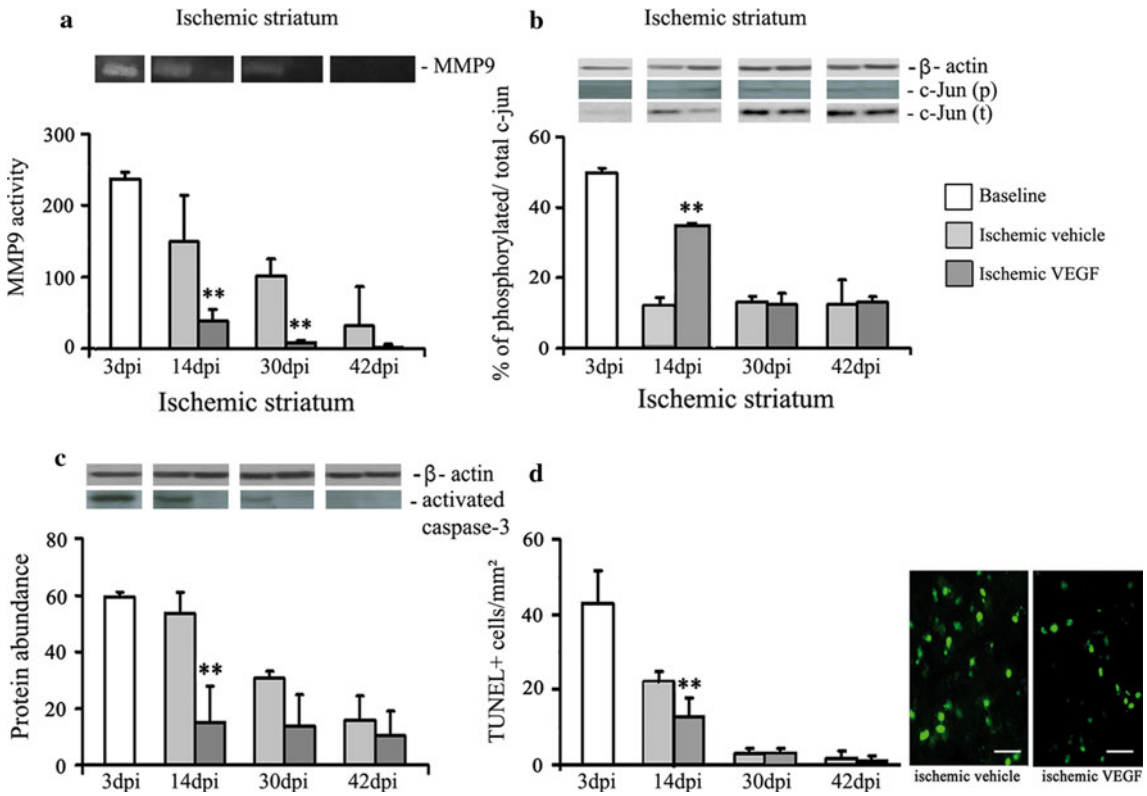

Fig. 5 VEGF deactivates MMP9, activates c-Jun and prevents caspase-3-dependent apoptotic cell death. Gelatin zymography for MMP9 (**a**), Western blot analysis using antibodies detecting total and phosphorylated c-Jun (**b**) and cleaved (i.e., activated) caspase-3 (**c**), as well as DNA fragmentation studies using TUNEL (**d**). For studies in (**a**)–(**c**), tissue samples obtained from the striatum were used. In (**b**) and (**c**), data are presented as optical densities. Protein loading was controlled with a β-actin antibody. Representative zymographies, blots and TUNEL stainings are shown. Data are means ± SD ($n = 3$ zymographies and western blots (**a**)–(**c**)/$n = 4$ animals per group). Data were analyzed by two-way ANOVA followed by two-tailed *t*-tests for individual time-points. $^{**}p < 0.01$ compared with vehicle-treated ischemic mice. *Bar* 45 μm

to exacerbate brain edema and neuronal injury when applied at early (1 h post ischemia) but not at late (48 h) time-points [34], thus pointing out a double-edged role of VEGF in the ischemic brain. The neuroprotective effect of VEGF involves the release of neurotrophic growth factors from cerebral microvascular cells [35] as well as direct neurotrophic effects of VEGF [15, 31].

Since VEGF promoted neuronal survival and angiogenesis, the question arose whether this enhanced neurovascular remodeling is accompanied by long-distance axonal plasticity in the ischemic hemisphere. Joint responses of vessels and axons to VEGF exposure could be expected based on observations during ontogeny, where angiogenesis and neuronal sprouting are closely linked. Throughout the periphery of the body, blood vessels and peripheral nerves share joint nerve and vessel sheaths, being navigated by very similar and partly overlapping growth and guidance cues [10]. Examples are members of the slit and semaphorin families that are involved in blood vessel and nerve guidance [2]. That axonal sprouting and angiogenesis were not jointly regulated by VEGF after stroke, like angiogenesis and neuronal survival, but spatially segregated from each other indicates that the responses of the adult CNS to injury differ from peripheral nerve-vessel systems.

In the induction of post-ischemic angiogenesis, MMPs, namely MMP9, play a crucial role. MMP9 contributes to the breakdown of the ECM, which prepares the stage for vascular growth. Following acute VEGF delivery, MMP9 activity increases in the perilesional ischemic tissue, closely in line with leaky vessels that are formed [26]. The brain response to chronic VEGF differs from acute VEGF delivery, as we now showed, since MMP9 was inhibited instead of activated by the growth factor. The deactivation of MMP9 may reflect the maturation of newly formed brain vessels. MMP9 has not only been involved in angiogenesis, but also in axonal remodeling and repair. By cleaving growth inhibitory proteins, such as the proteoglycan NG2, MMP9 was suggested to promote axonal myelination. As such, impaired remyelination was observed in MMP9 deficient mice in a model of lysolecithin-induced demyelination [16], which was interpreted as a consequence of the lack of proteoglycan proteolysis. It is conceivable that the deactivation of MMP9 contributed to the lack of axonal

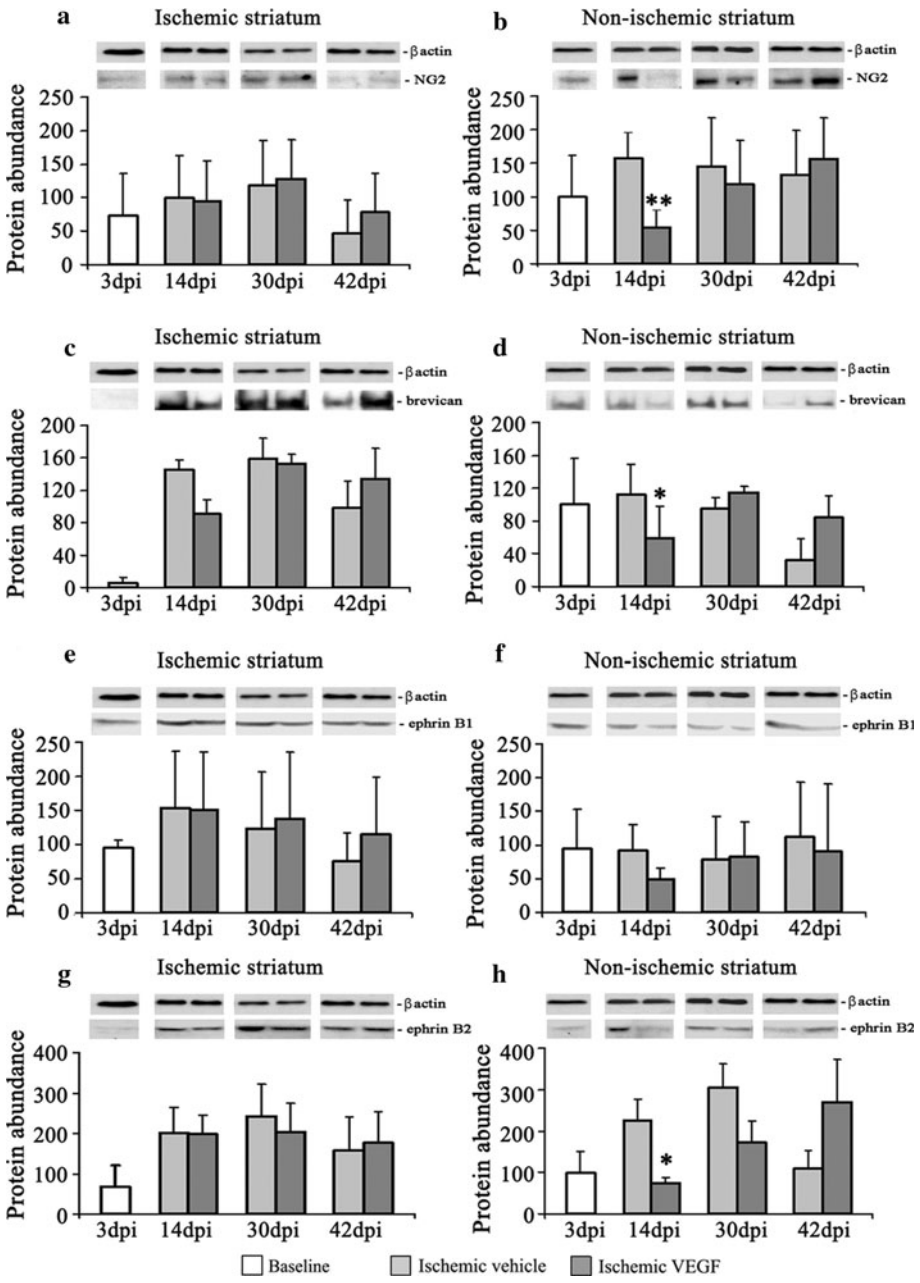

Fig. 6 VEGF downregulates growth inhibitory proteoglycans and guidance molecules in the contralesional hemisphere. Western blot analysis using antibodies detecting total NG2 proteoglycan (**a**, **b**), brevican (**c**, **d**), ephrin B1 (**e**, **f**) and ephrin B2 (**g**, **h**), both for the ischemic and contralesional non-ischemic striatum. Note the downregulation of the proteoglycans and guidance molecules in the contralesional non-ischemic striatum at 14 dpi. Data were normalized with values determined in the contralateral striatum of animals submitted to focal cerebral ischemia followed by 3 days reperfusion. Protein loading was controlled with a β-actin antibody. Representative blots are shown. Data are means ± SD ($n = 3$ western blots). Data were analyzed by two-way ANOVA followed by two-tailed *t*-tests. $*p < 0.05$/ $**p < 0.01$ compared with non-ischemic vehicle

sprouting in the lesioned hemisphere by preventing the degradation of growth-inhibitory glycoproteins, thus resulting in a reduced permissiveness of the ECM for growing axons. That the breakdown of ECM glycoproteins by MMP9 is indeed required so that successful brain remodeling may take place, has already been shown by Zhao et al. [36] in rats submitted to focal cerebral ischemia. In their study, the authors prevented ECM breakdown by means of MMP inhibitors and observed increased brain injury, disturbed angiogenesis and impaired neurological recovery.

With respect to the axonal plasticity contralateral to the stroke, the transient downregulation of the axonal growth inhibitors NG2 and brevican and of the guidance molecules ephrin B1 and ephrin B2 in the contralesional hemisphere offers important clues. Ephrins, namely ephrin B2, are required for developmental as well as tumor-associated angiogenesis, promoting the internalization of VEGF receptors, namely VEGFR2 that mediates angiogenesis, into cells [20, 28]. Internalization of VEGFR2 is necessary for activation and downstream signaling of the receptor and is needed for the VEGF-induced extension of the cells, which sets the stage for vessel sprouting [20]. Intriguingly, the effects of ephrins on axons differ from those on vessels. During development, ephrins may have attractant and repellent properties, depending on their site of action and

the coexpression of ephrin receptors [12]. In the adult brain, on the other hand, the primary role of ephrins in regeneration is repulsive [10]. From this perspective, the downregulation of ephrin B2 and ephrin B1 similar as that of NG2 and brevican may have created a favorable environment, in which pyramidal tract plasticity became possible. Further studies will be necessary to better delineate the structural, molecular and functional processes underlying lesion-remote plasticity after stroke.

Acknowledgments The authors would like to thank Prof. Martin E. Schwab, Brain Research Institute, University of Zurich, for sharing his expertise regarding the use of anterograde tract tracers in the evaluation of corticobulbar axonal plasticity. The authors would like to thank Beate Karow for technical assistance. This work was supported by grants of the German Research Foundation (HE3173/2-1 and 3173/3-1; to D.M.H.), a Dr. Werner Jackstädt Foundation fellowship (to R.R.) and an endowment of the Heinz Nixdorf Foundation (to D.M.H.).

References

1. Andrews EM, Tsai SY, Johnson SC et al (2008) Human adult bone marrow-derived somatic cell therapy results in functional recovery and axonal plasticity following stroke in the rat. Exp Neurol 211:588–592
2. Autiero M, De Smet F, Claes F, Carmeliet P (2005) Role of axonal quidance signals in blood vessel navigation. Cardiovasc Res 65:629–638
3. Bacigaluppi M, Pluchino S, Peruzzotti-Jametti LP et al (2009) Delayed post-ischemic neuroprotection following systemic neural stem cell transplantation involves multiple mechanisms. Brain 132:2239–2251
4. Buchli AD, Schwab ME (2005) Inhibition of Nogo: a key strategy to increase regeneration, plasticity and functional recovery of the lesioned central nervous system. Ann Med 37:556–567
5. Cramer SC, Chopp M (2000) Recovery recapitulates ontogeny. Trends Neurosci 23:265–271
6. Ding G, Jiang Q, Li L, Zhang L et al (2008) Magnetic resonance imaging investigation of axonal remodeling and angiogenesis after embolic stroke in sildenafil-treated rats. J Cereb Blood Flow Metab 28:1440–1448
7. ElAli A, Hermann DM (2010) Apolipoprotein E controls ATP-binding cassette transporters in the ischemic brain. Sci Signal 3:ra72
8. Forsythe JA, Jiang BH, Iyer NV, Leung SW, Koos RD, Semenza GL (1996) Activation of vascular endothelial growth factor gene transcription by hypoxia-inducible factor 1. Moll Cell Biol 16:4604–4613
9. Gerloff C, Bushara K, Sailer A et al (2006) Multimodal imaging of brain reorganization in motor areas of the contralesional hemisphere of well recovered patients after capsular stroke. Brain 129:791–808
10. Giger RJ, Hollis ER 2nd, Tuszynski MH (2010) Guidance molecules in axonal regeneration. Cold Spring Harb Perspect Biol 2: a001867
11. Hermann DM, Zechariah A (2009) Implications of vascular endothelial growth factor for postischemic neurovascular remodelling. J Cereb Blood Flow Metab 29:1620–1643
12. Hindges R, McLaughlin T, Genoud N, Henkenmeyer M, O'Leary DD (2002) EphB forward signaling controls directional branch extension and arborization required for dorsal-ventral retinotopic mapping. Neuron 35:475–487
13. Kilic E, Spudich A, Kilic Ü et al (2008) ABCC1: a gateway for pharmacological compounds to the ischaemic brain. Brain 131:2679–2689
14. Kilic E, ElAli A, Kilic Ü et al (2010) Role of Nogo-A in neuronal survival in the reperfused ischemic brain. J Cereb Blood Flow Metab 30:969–984
15. Kilic Ü, Kilic E, Järve A et al (2006) Human vascular endothelial growth factor protects axotomized retinal ganglion cells in vivo by activating ERK-1/2 and Akt pathways. J Neurosci 29:12439–12446
16. Larsen PH, Wells JE, Stallcup WB, Opdenakker G, Yong VW (2003) Matrix metalloproteinase-9 facilitates remyelination in part by processing the inhibitory NG-2 proteoglycan. J Neurosci 23:11127–11135
17. Monacci WT, Merrill MJ, Oldfield EH (1993) Expression of vascular permeability factor/vascular endothelial growth factor in normal rat tissues. Am J Physiol 164:C995–C1002
18. Papadopoulos CM, Tsai S-Y, Alsbiei T, O'Brien TE, Schwab ME, Kartje GL (2002) Functional recovery and neuroanatomical plasticity following middle cerebral artery occlusion and IN-1 antibody treatment in the adult rat. Ann Neurol 51:435–441
19. Reitmeir R, Kilic E, Kilic Ü et al (2011) Post-acute delivery of erythropoietin induces stroke recovery by promoting peri-lesional tissue remodeling and contralesional pyramidal tract plasticity. Brain 135:84–99
20. Sawamiphak S, Seidel S, Essmann CL et al (2010) Ephrin-B2 regulates VEGFR2 function in developmental and tumor angiogenesis. Nature 465:487–491
21. Stowe AM, Plautz EJ, Eisner-Janowicz I et al (2007) VEGF protein associates to neurons in remote regions following cortical infarct. J Cereb Blood Flow Metab 27:76–85
22. Stowe AM, Plautz EJ, Nguyen P et al (2008) Neuronal HIF-1 alpha protein and VEGFR-2 immunoreactivity in functionally related motor areas following a focal M1 infarct. J Cereb Blood Flow Metab 28:612–620
23. Sun Y, Jin K, Xie L et al (2003) VEGF-induced neuroprotection, neurogenesis and angiogenesis after focal cerebral ischemia. J Clin Invest 111:1843–1851
24. Sugiura S, Kitagawa K, Tanake S et al (2005) Adenovirus-mediated gene transfer of heparin-binding epidermal growth factor-like growth factor enhances neurogenesis and angiogenesis after focal cerebral ischemia in rats. Stroke 36:859–864
25. Tremml P, Lipp HP, Müller U, Ricceri L, Wolfer DP (1998) Neurobehavioral development, adult openfield exploration and swimming navigation learning in mich with a modified beta-amyloid precursor protein gene. Behav Brain Res 95:65–76
26. Valable S, Montaner J, Bellail A et al (2005) VEGF-induced BBB permeability is associated with an MMP-9 activity increase in cerebral ischemia: both effect decreased by ANG-1. J Cereb Blood Flow Metab 25:1491–1504
27. Van der Zijden JP, Bouts MJ, Wu O (2008) Manganese-enhanced MRI of brain plasticity in relation to functional recovery after experimental stroke. J Cereb Blood Flow Metab 28:832–840
28. Wang Y, Nakayama M, Pitulescu ME et al (2010) Ephrin-B2 controls VEGF-induced angiogenesis and lymphangiogenesis. Nature 465:483–486
29. Wang Y, Kilic E, Kilic Ü et al (2005) VEGF overexpression induces post-ischemic neuroprotection, but facilitates haemodynamic steal phenomena. Brain 128:52–63
30. Wang Y-Q, Guo X, Qiu M-H, Feng X-Y, Sun F-Y (2007) VEGF overexpression enhances striatal neurogenesis in brain of adult rat after a transient middle cerebral artery occlusion. J Neurosci Res 83:73–82

31. Wick A, Wick W, Waltenberger J, Weller M, Dichgans J, Schulz JB (2002) Neuroprotection by hypoxic preconditioning requires sequential activation of vascular endothelial growth factor receptor and Akt. J Neurosci 22:6401–6407
32. Wiessner C, Bareyre FM, Allegrini PR et al (2003) Anti-Nogo-A antibody infusion 24 hours after experimental stroke improved behavioral outcome and corticospinal plasticity in normotensive and spontaneously hypertensive rats. J Cereb Blood Flow Metab 23:154–165
33. Zea Longa EL, Weinstein PR, Carlson S, Cummins R (1989) Reversible middle cerebral artery occlusion without craniectomy in rats. Stroke 20:84–91
34. Zhang ZG, Zhang L, Jiang Q et al (2000) VEGF enhances angiogenesis and promotes blood-brain barrier leakage in the ischemic brain. J Clin Invest 106:829–838
35. Zhang ZG, Chopp M (2009) Neurorestaurative therapies for stroke: underlying mechanisms and translation to the clinic. Lancet Neurol 8:491–500
36. Zhao BQ, Wang S, Kim H-Y, Storrie H, Rosen BR, Mooney DJ et al (2006) Role of matrix metalloproteinases in delayed cortical responses after stroke. Nat Med 12:441–445
37. Z'Graggen WJ, Metz GA, Kartje GL, Thallmair M, Schwab ME (1998) Functional recovery and enhanced corticofugal plasticity after unilateral pyramidal tract lesion and blockade of myelin-associated neurite growth inhibitors in adult rats. J Neurosci 18:4744–4757